DOI: 10.7860/IJARS/2021/46182:2721

Review Article

Radiology Section

Imaging in Spinal Dysraphism- A Pictoral Assay

ANURUDH KISHORE VATTI[1], SWARNALATHA SEELAM[2], VINEELA REKHA VIDAVALURU[3]

ABSTRACT

Spinal dysraphism includes the congenital malformations of the spine and spinal cord. Spinal cord development takes place through successive stages of gastrulation, primary neurulation, and secondary neurulation. Defect in any of these three phases can lead to spinal dysraphism. The embryological classification of spinal dysraphism consists of anomalies of gastrulation, anomalies of primary neurulation, combined anomalies of gastrulation, primary neurulation and anomalies of secondary neurulation. Clinico-radiologic classification of spinal dysraphism consists of open and closed types. Magnetic Resonance Imaging (MRI) is considered as the gold standard for identifying these disorders. By using the clinical, neuroradiological, and development data systematically an accurate diagnosis can be reached. In this article, authors revise the normal development of the spinal cord and spine and discuss the embryologic classification by illustrating the diverse MRI findings of various spinal dysraphism.

Keywords: Congenital malformations, Gastrulation, Magnetic resonance imaging, Primary neurulation, Secondary neurulation

INTRODUCTION

Spinal dysraphism includes the congenital abnormalities of the spine and spinal cord. Abnormal midline closure of bony, mesenchymal, and nervous tissue leads to the formation of these heterogeneous groups of anomalies [1]. The usual age at diagnosis is at birth or early infancy but few are detected at a later age due to the absence of clinical manifestations. The inherent advanced soft-tissue resolution and multiparametric imaging capability of MRI allow easier, rapid, and more precise diagnosis of these disorders, thus enabling early detection and case-tailored management [2]. By analysis of the clinical, neuroradiological, and development data systematically, an accurate diagnosis can be reached.

EMBRYOLOGY (A QUICK RECAP OF SPINAL CORD DEVELOPMENT)

Spinal cord development occurs in three basic embryologic steps [3,4]. They include gastrulation (2-3 weeks), primary neurulation (3-4 weeks) and secondary neurulation (5-6 weeks). In gastrulation, the embryonic disc from a bilaminar disc is transformed into a trilaminar dics (composed of ectoderm, mesoderm and endoderm) [Table/Fig-1a,b] [5]. In primary neurulation, notochord and overlying ectoderm interact to form neural plate. The neural plate then arches, folds and closes in a zipper like manner birectionally to form the neural tube [Table/Fig-2a,b] [5]. In secondary neurulation, secondary neural tube is formed from caudal cell mass, which is solid initially and subsequently undergoes cavitation.It forms tip of conus medullaris and filum terminale by retrogressive differentiation [Table/Fig-3a-c] [5]. Abnormalities in any of the above stages can lead to spine and spinal cord malformations.

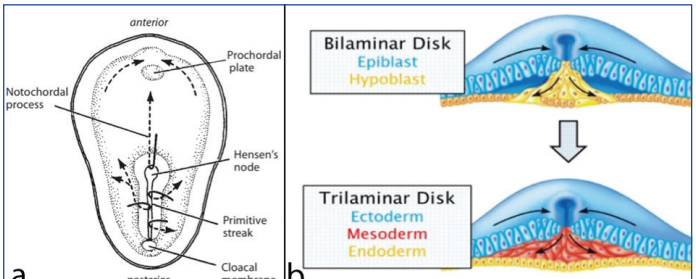

[Table/Fig-1]: Gastrulation. a) Dorsal view and b) Transverse view of the bilaminar embryonic disk. First ingressing cells at Hensen's node move anterior to form head processes and notochord. Cells ingressing through primitive streak migrate ventrally and laterally to form mesodermal and endodermal precursors [5].

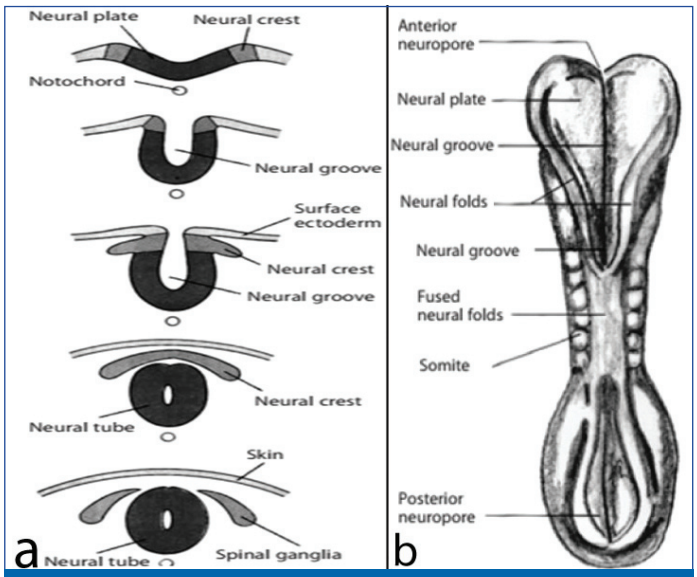

[Table/Fig-2]: Primary neurulation. a) Set of transverse views shows evolution from flat neural plate to fused neural tube. Also notice disjunction of the neural ectoderm from the surface ectoderm at the time of neural tube fusion; b) Dorsal view of the embryo on gestational day 21 shows fusion of the neural folds to form a neural tube has begun at the cervical level and proceeds bidirectionally [5].

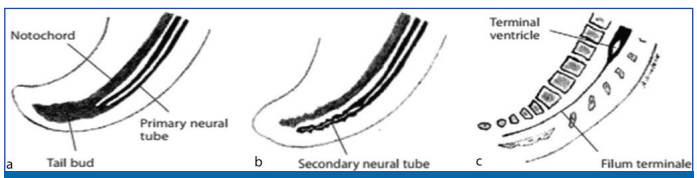

[Table/Fig-3]: Secondary neurulation. a) The tail bud forms as a result of coalescence of the neuroectoderm with the lower notochord; b) A secondary neural tube connects cranially with the neural tube formed by primary neurulation; c) Eventually, the tip of the conus medullaris and the filum terminale result from this process. The terminal ventricle is the sole remnant of the secondary neural canal.

PREDISPOSING FACTORS

- Nutritional factors: Cytochalasin ingestion, a metabolite of the fungus Phytophthora infestans (found in blighted potatoes),

deficiency of folic acid or zinc, high nitrates (eg, nitrate-cured meats, bore and ground water), and deficiency or excess vitamin A [6,7].

- Multifactorial with genetic (Chromosomal and single-gene abnormalities) and environmental factors playing a role [8].
- An altered carbohydrate metabolism has been reported in mothers of children with spinal dysraphism, especially those with sacral agenesis [9].
- In consanguineous marriage there is a 3-fold increased incidence and more in monozygotic twins. There is 50% likelyhood of 2nd child being affected if the first child is affected and 100% likelyhood if two children are affected [10].

INCIDENCE

Spinal dysraphism affect approximately 1 per 1000 live-born infants. Open spinal dysraphism occur more frequently than closed and among the open type, myelomeningocele is the most common [8].

CLASSIFICATION

Based on studies by Tortori and Caffey, spinal dysraphism is classified according to the embryological events [Table/Fig-4] [4,11,12].

1. Anomalies of Gastrulation
A. Disorders of notochord formation
Caudal regression syndrome
Segmental spinal dysgenesis
B. Disorders of notochord integration
Neurenteric cysts
Dorsal enteric fistula
Split cord malformations [diastematomyelia]
2. Anomalies of Primary Neurulation
A. Premature dysjunction
Lipomyelomeningocele
Lipomyelocele
Intradural lipoma
B. Nondysjunction
Dorsal dermal sinus
Myelomeningocele
Myelocele
3. Combined Anomalies of Gastrulation and Primary Neurulation
Hemimyelocele
Hemimyelomeningocele
4. Anomalies of Secondary Neurulation and Retrogressive Differentation
Abnormally long spinal cord
Persistent terminal ventricle
Tight filum terminale
Intrasacral-anterior sacral meningocele
Terminal myelocystocele

[Table/Fig-4]: Embryological classification of spinal dysraphism [4,11,12].

Clinico-radiologically, based on the presence of overlying skin, spinal dysraphism is classified as open and closed types [13-15]. Overlying skin is absent and the neural elements are exposed to the external environment in open type while, in closed type, the skin is intact. Based on the presence of subcutaneous mass closed spinal dysraphism can be further divided [Table/Fig-5,6].

Open spinal dysraphisms
*Myelomeningocele
*Myelocele
*Hemimyelmeningocele
*Hemimyelocele
Closed spinal dysraphism
With subcutaneous mass
*Lipomyelomeningocle
*Lipomyelocele
*Terminal myelocystocele
*Meningocele
*Myelocystocele
Without cutaneous mass
*Simple dysraphic states
*Intradural lipoma
*Filar lipoma
*Tight filum terminale
*Persistent terminal ventricle
*Dorsal dermal sinus
Complex dysraphic states
*Dorsal enteric fistula
*Neuroentiric cyst
*Diastomatomyelia
*Caudal agenesis
*Segmental spinal dysgenesis

[Table/Fig-5]: Clinico-radiological Classification of spinal dysraphisms.

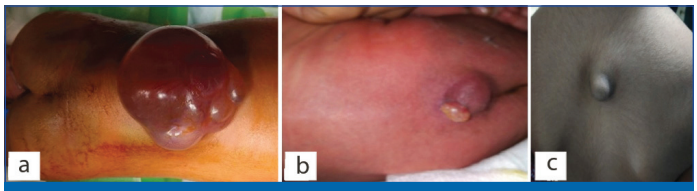

[Table/Fig-6]: Clinical images of open (a,b) and closed (c) spinal dysraphism.

1. GASTRULATION RELATED ABNORMALITIES

The spinal cord and various structures derived from notochord are affected by abnormal gastrulation [16]. Most of these abnormalities are covered by skin and with no subcutaneous mass. Disorders of midline notochordal integration and disorders of notochordal formation come under this category.

A. Disorders of Notochordal Formation

Caudal agenesis and segmental spinal dysgenesis are disorders of notochordal formation and occur as a result of abnormal apoptosis [17].

Caudal agenesis (CA): It may lead to total or partial agenesis of the spinal column. Commonly associated other anomalies are the genital anomalies, pulmonary hypoplasia, anal imperforation, renal aplasia or dysplasia, and limb abnormalities. CA is divided into two types:

Type I CA: Caudal cell mass and notochord formation are affected. There are high position and abnormal termination of conus medullaris(most commonly at the level of D12 vertebra). Vertebral aplasia of varying degree is seen.

Type II CA: Only caudal cell mass is affected while notochord formation is unaffected. Hence, only secondary neurulation is defective with normal primary neurulation. Consequently, only the caudal part of conus medullaris is absent. Vertebral dysgenesis is less severe. Patients present with tethered cord syndrome as the conus in these cases is stretched and tethered [18,19].

Segmental spinal dysgenesis: It is a rare notochordal abnormality occurring due involvement of the intermediate segment of notochord during gastrulation [Table/Fig-7,8] [17,20]. Characterised by segmental agenesis or dysgenesis of the lumbar or thoracolumbar spine and spinal cord or nerve roots. The child presents with congenital paraparesis or paraplegia with or without associated congenital lower limb deformities.

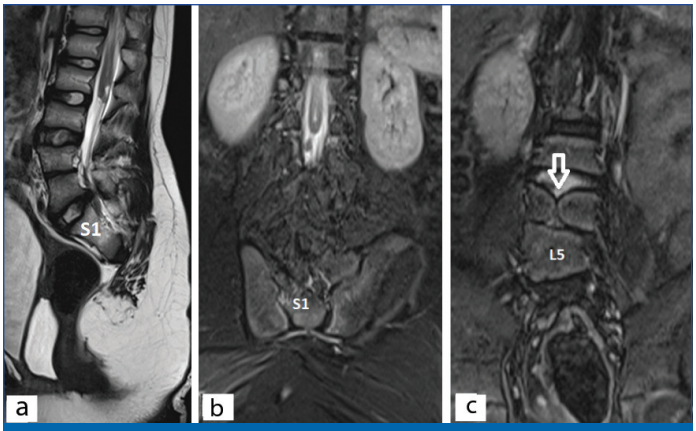

[Table/Fig-7]: Total sacral agenesis- Sagittal T2 weighted (a) Coronal T2 STIR (b) Images of lumbosacral spine show complete agenesis of sacrum and coccyx distal to S1 vertebra. Coronal T2 STIR (c) Image demonstrates L4 butterfly vertebra (arrow).

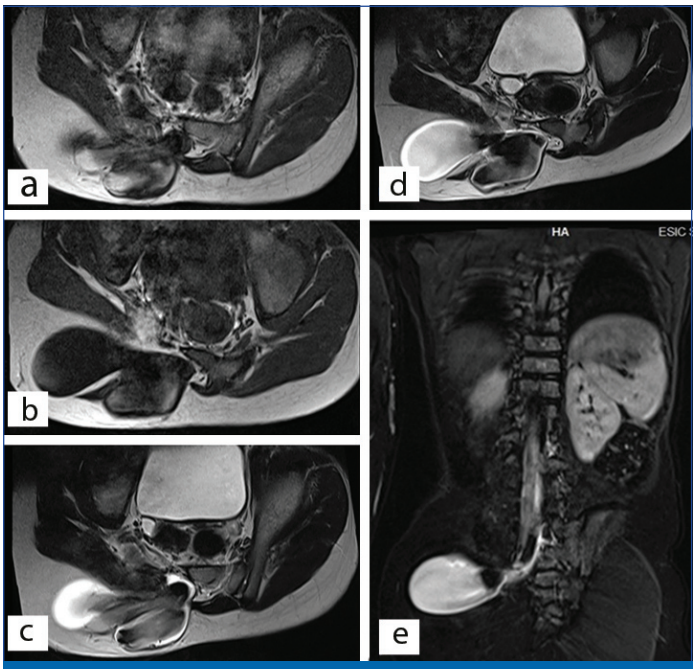

[Table/Fig-8]: Right hemisacral agenesis with lipomyelomeningocele- Axial T1 weighted (a,b) Axial T2 weighted (c,d) and Coronal T2 STIR (e) Images show absent formation of right hemisacrum with herniation of meninges and neural elements into right gluteal region forming a placode-lipoma interface outside the spinal canal. The overlying skin covering is intact

B. Disorders of Midline Notochordal Integration

Midline notochordal integration is a process where paired notochord anlagen fuse to form a single midline notochord process [3]. Longitudinal splitting of the spinal cord occurs due to abnormality in this step. Neurenteric cyst and diastematomyelia are the common entities of this category.

Neurenteric cyst: Dorsalenteric fistula is a persistent communication between ectoderm (External skin) and endoderm (Intestine).Among disorders of midline notochord integration it is the rare and most severe form. It is a persistent communication between ectoderm (skin surface) and endoderm (bowel). Neuroenteric cysts are trapped remnants of the middle portion of this communication. It is a localised form of dorsal enteric fistula. They are usually intradural and extramedullary in location. Most commonly located in the cervicothoracic region, may be seen in other locations also [21]. They are present anterior to the cervical spinal cord with associated adjacent vertebral anomalies. On T1 and T2 weighted MR images, they appear isointense to hyperintense to CSF (due to high protein content) with absent contrast enhancement [22,23].

Diastematomyelia: Defective midline notochord integration leads to a single midline notochord being replaced by a paired notochordal process which are separated by intervening primitive streak cells. Each "heminotochord" induces a separate "hemi"-neural plate. Each "Hemi"-neural plate, in turn, forms a "Hemi"-neural tube, thus resulting in the formation of two hemicords. The intervening primitive streak tissue, which is a totipotent tissue decides the type of diastematomyelia. In type I diastematomyelia,it differentiates into cartilage and bone,so the two hemicords lie in individual dural sacs separated by osteocartilagenous spur [Table/Fig-9,10]. Whereas in type II diastematomyelia,it is resorbed,so the single dural sac encases the two hemicords [Table/Fig-11,12] [24]. Associated vertebral anomalies and hydromyelia may be present. One of the reliable clinical indicators for underlying diastematomyelia is the presence of a high lying hairy tuft over a child's back [25].

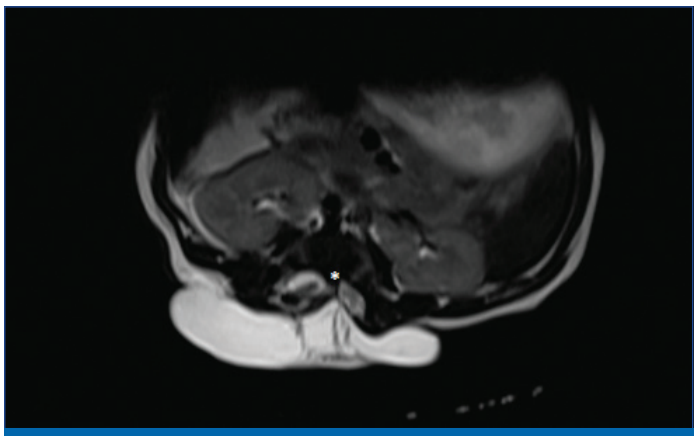

[Table/Fig-9]: Type 1 Diastematomyelia- axial T2 weighted MR image shows two dural tubes separated by osseous bridge (*) at L1 vertebral level.

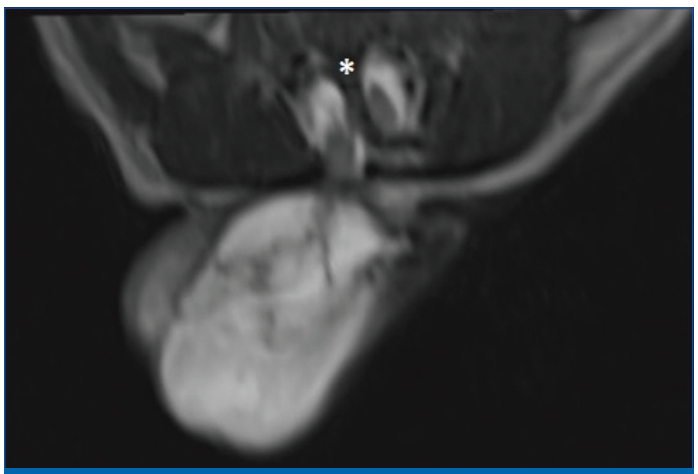

[Table/Fig-10]: Type 1 Diastematomyelia- axial T2 weighted MR image shows two dural tubes separated by osseous bridge (*).

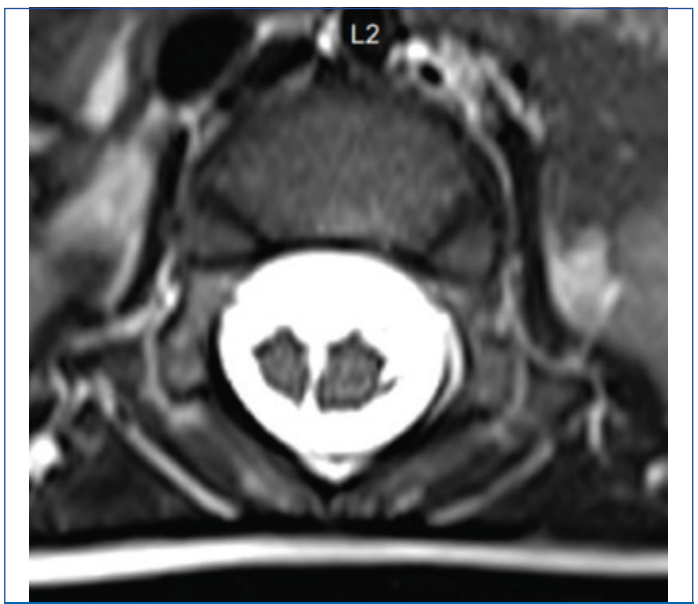

[Table/Fig-11]: Type 2 Diastematomyelia- axial T2 weighted MR image show splitting of distal cord into two hemicords within single dural tube.

[Table/Fig-12]: Type 2 Diastematomyelia-Axial USG image of spinal canal at L2 level showing splitting of distal spinal cord into two hemicords.

2. PRIMARY NEURULATION RELATED ABNORMALITIES

A. Premature Dysjunction

Premature dysjunction of the neural tube from the overlying ectoderm leads to the interposition of perineural mesenchyme between the neural tube and ectoderm, which differentiates into fat and prevents complete neural tube closure. The lipomatous malformation spectrum of lipomyelocele, lipomyelomeningocele, and spinal lipomas come under this category [11].

Lipomyelocele and lipomyelomeningocele: Lipomyelocele and lipomyelomeningocele fall under the category of lipomas with a dural defect. As a consequence of premature focal disjunction of the neural tube from the surface ectoderm, the mesenchymal tissue intrudes into the neural tube. The adipomatous tissue is formed from this mesenchymal tissue due to factors not known [26]. Patients present clinically with a subcutaneous swelling above the intergluteal crease. The major distinguishing feature between the lipomyelocele and lipomyelomeningocele is the location of the neural placode-lipoma interface. It is situated within the spinal canal in a lipomyelocele [Table/Fig-13], while in lipomyelomeningocele it is situated outside the spinal canal as a consequence of the expansion of the subarachnoid space [Table/Fig-14,15] [14]. T1 and T2 weighted images show the continuity between the dorsal surface of placode with subcutaneous fat, with signal suppression on the fat-saturated images.

Intradural lipoma: It is a lipoma situated on the midline dorsal aspect of the spinal cord within an unbreached dural sac. The unbreached dural sac distinguishes it from lipomyelocele and lipomyelomeningocele. Lumbosacral region is the most common site of location and tethered cord syndrome is the most common clinical presentation. On MRI, they have a signal intensity similar to subcutaneous fat on all the sequences [13].

Filar lipoma: It is the fibrolipomatous thickening of the filum terminale. It follows the signal intensity of fat on all the MR sequences [12]. It is considered a normal variant unless associated with tethered cord syndrome [27,28].

B. Nondysjunction

Failure of separation of the neural tube from overlying ectoderm results in an ectoderm-neuroectoderm communication that blocks the mesenchymal migration. As a consequence, the open neural tube defect spectrum of the dorsal dermal sinus, myelomeningocele, and meningocele is formed.

Dorsal dermal sinus: It is an epithelium lined fistulous tract connecting neural tissue or meninges with the cutaneous surface. Lumbosacral region is the most common site of location. They are commonly

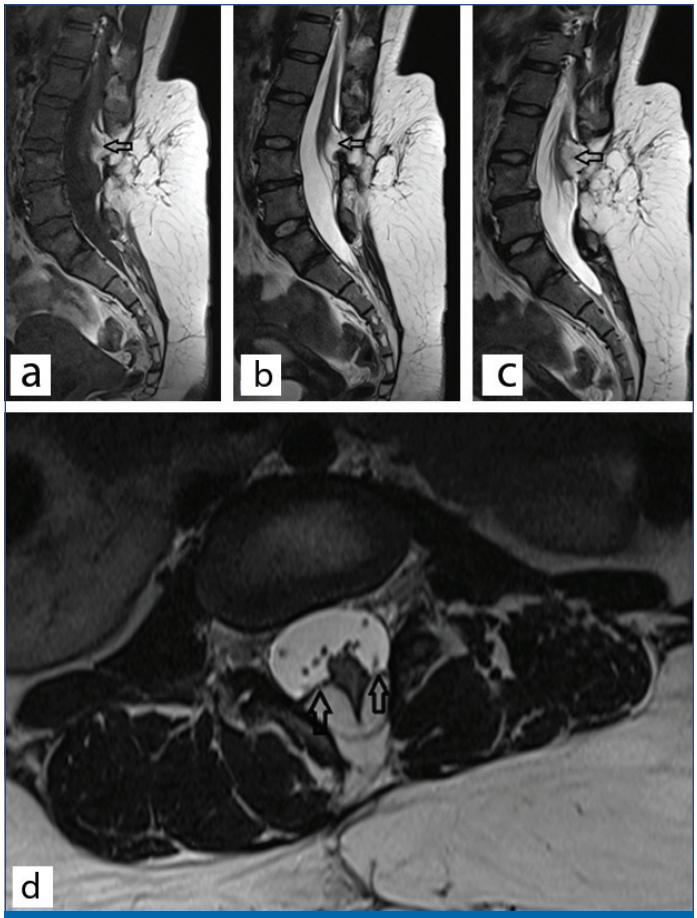

[Table/Fig-13]: Lipomyelocele- Sagittal T1 (A), Sagittal T2 (B,C) and axial T2 images (D) of lipomyelocele shows placode-lipoma interface lying within spinal canal (arrow).

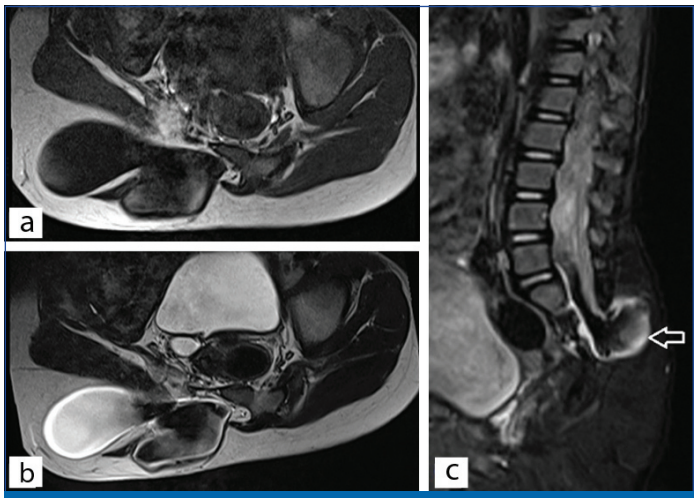

[Table/Fig-14]: Lipomyelomeningocele- Axial T1 weighted (a) and axial T2 weighted images (b) of lipomyelomeningocele shows placode- lipoma interface (arrow) lying outside the spinal canal due to expansion of subarachnoid space. There is suppression of lipoma at interface as seen on Saggital T2 STIR images (c). Overlying skin is intact.
Absent formation right hemisacrum (Right hemisacral agenesis)

associated with an intraspinal dermoid cyst. Patients present clinically with cutaneous markers like hairy nevus, midline dimple, or capillary hemangioma [29]. Meningitis is the most severe complication due to the presence of external communication.

Myelomeningocele and myelocele: Myelomeningocele and myelocele are the open neural tube defects in which the neural placode is exposed through the midline skin defect on the back. Myelomeningocele constitutes 98% of all the open spinal dysraphism. In myelomeningocele the neural placode extrudes above the skin surface, presenting clinically as a midline reddish mass [3]. Myelocele is a rare anomaly. The major distinguishing feature between myelomeningocele and myelocele is the position of the neural placode. In myelocele, it is flush with the skin surface

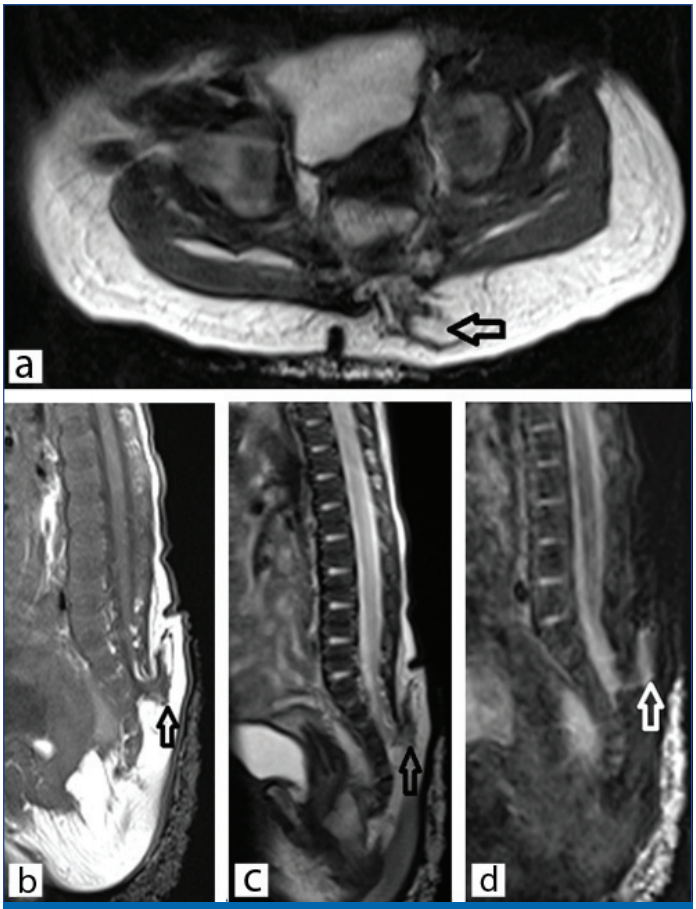

[Table/Fig-15]: Lipomyelomeningocele- Axial T1 Weighted (a) Sagittal T1 weighted (b) Saggital T2 Weighted (c) images of lipomyelomeningocele shows placode-lipoma interface (arrow) lying outside the spinal canal due to expansion of subarachnoid space. (d) There is suppression of lipoma at interface as seen on saggital T2 STIR images.

[Table/Fig-16], but extrudes over the skin surface due to expansion of the subarachnoid space in myelomeningocele [Table/Fig-17-19] [30]. Almost all the patients have an associated Chiari II malformation and about 80% have hydrocephalus [Table/Fig-20] [3,4].

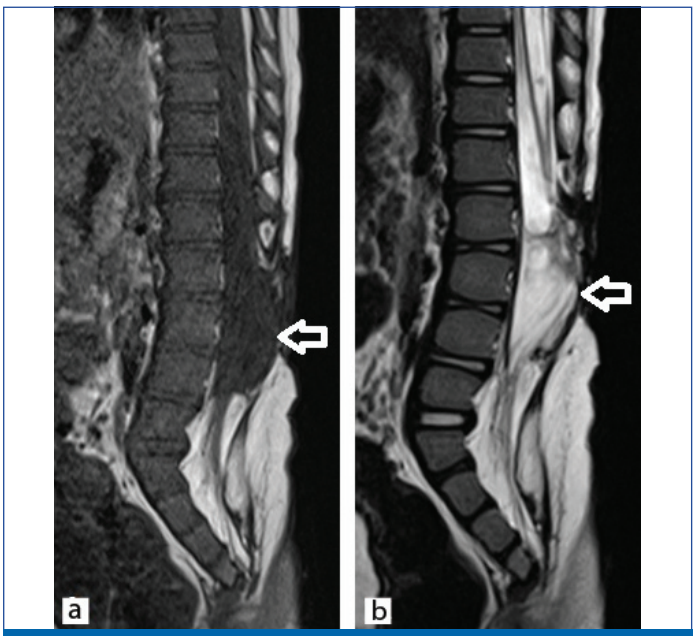

[Table/Fig-16]: Myelocele-Sagittal T1 weighted (a), Sagittal T2 Weighted (b) Images of dorsolumbar spine in a case of myelocele showing the neural placode flush with the skin surface (arrow). Skin covering is absent over the myelocele.

3. COMBINED ANOMALIES OF GASTRULATION AND PRIMARY NEURULATION

Hemimyelomeningocele and hemimyelocele

Hemimyelomeningoceles and hemimyeloceles are remarkably rare anomalies. They occur when a myelomeningocele or myelocele

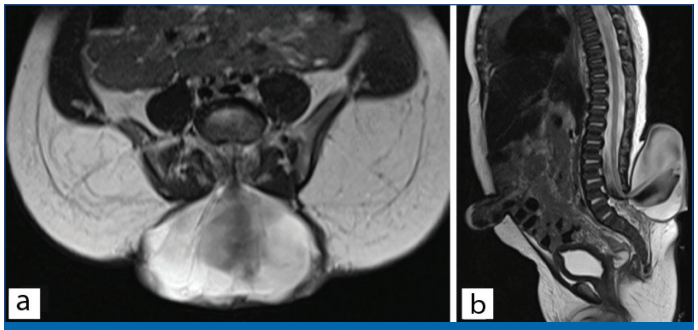

[Table/Fig-17]: Lumbo-sacral Myelomeningocele- Axial T2 weighted (a) Sagittal T2 weighted (b) Images show low lying cord with neural placode protruding above skin surface due to expansion of underlying subarachnoid space.
Midline anterior abdominal wall defect at umbilicus with herniation of bowel loops-S/O Omphalocele

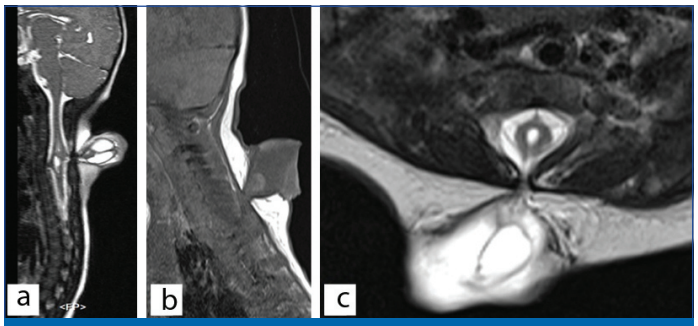

[Table/Fig-18]: Cervical Myelomeningocele -T2 weighted sagittal (a), T1 weighted sagittal (b) and T2 weighted axial (c) images of cervical spine showing myelomeningocele. There is posterior herniation of a CSF filled sac containing nerve fibers. Spinal cord show kinking at the same level and dilated central canal suggestive of syringohydromyelia. There is no overlying skin.

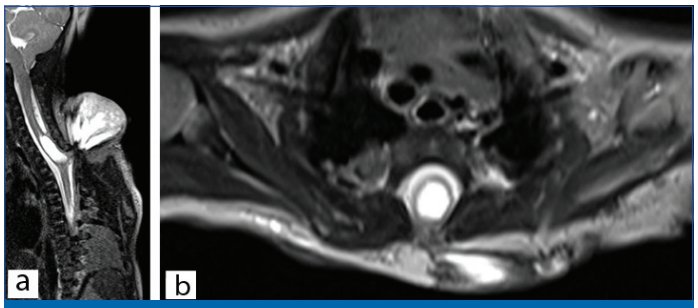

[Table/Fig-19]: Cervico-Dorsal Myelomeningocele -T2 Fatsat sagittal (a) T2 weighted axial (b) Images of cervico-dorsal spine showing myelomeningocele. There is posterior herniation of a CSF filled sac containing nerve fibers. Spinal cord show kinking at the same level and dilated central canal suggestive of syringohydromyelia. There is no overlying skin.

are associated with diastematomyelia and one hemicord fails to neurulate [Table/Fig-21,22].

4. ANOMALIES OF SECONDARY NEURULATION/ANOMALIES OF THE CAUDAL CELL MASS

Low lying cord: Spinal cord position below L2-L3 level after the first month in a term infant is “abnormally low lying”. Axial T1 weighted images are used for knowing the actual position of the conus [31].

Persistent terminal ventricle/fifth ventricle: It is the small ependymal lined cavity within the conus medullaris. It is the reminant of the lumen of the neural tube formed by the secondary neurulation. Absent contrast enhancement and the location just above filum terminale are the characteristic imaging findings and distinguish it from other cystic lesions of conus medullaris [Table/Fig-23] [32].

Tethered Cord Syndrome (TCS): Clinical manifestations included in TCS are gait spasticity, low back pain, leg pain, sensory abnormalities of the lower extremity, and/or bladder abnormalities. A low lying cord with thick filum terminale (>1.5 mm) is the key imaging finding [Table/Fig-24].

Intrasacral-anterior sacral meningocele: It is the arachnoid lined sac located in the enlarged sacral spinal canal. It is connected to the

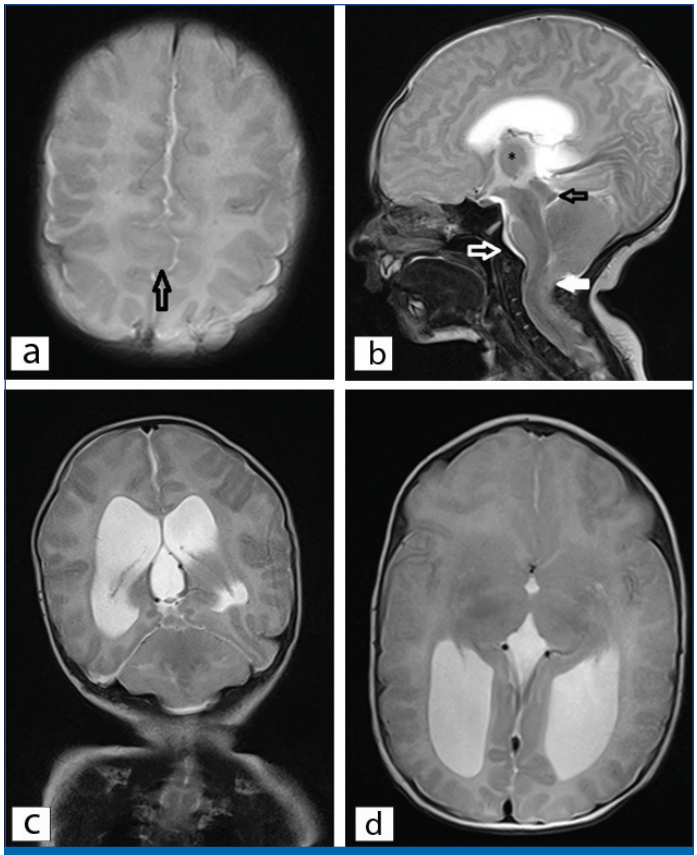

[Table/Fig-20]: Features of Chiari II malformation; a) Axial T2 Weighted image shows hypoplastic,fenestrated falx cerebri with interdigitating gyri (arrow); b) Sagittal T2 Weighted image shows elongated tube like fourth ventricle,"cascade" of inferiorly displaced vermis behind the medulla (Bold white arrow), large massa intermedia (*), tectal beaking (Black arrow) and concave clivus (Thin white arrow); c) Coronal T2 Weighted image shows small posterior fossa with dilated lateral and third ventricle suggesting of Hydrocephalus; d) Axial T2 Weighted image depicts enlargement of the occipital horns of the lateral ventricles (arrow) due to hydrocephalus.

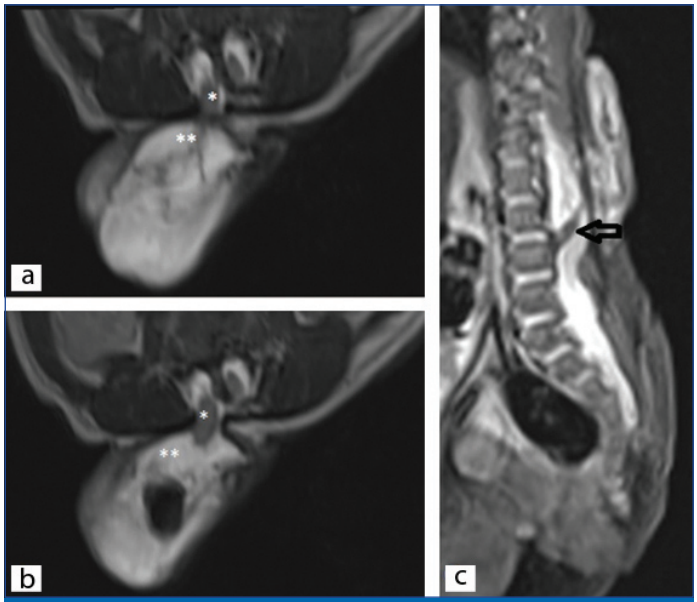

[Table/Fig-21]: Hemimyelomeningocele- Axial T2 weighted (a,b) and sagittal T2 fatsat (c) images shows type 1 diastometamyelia with the right hemicord (*) seen ending within a myelomeningocele sac (**).
Note the bony spur (arrow in C)

caudal end of the dural sac by an opening that allows the passage of CSF from the subarachnoid space.

CONCLUSION(S)

Congenital malformations of the spine and spinal cord have a complex and variable imaging appearance. A meticulous approach with consideration of clinical, developmental data along with the proper interpretation of imaging findings helps in precise diagnosis.

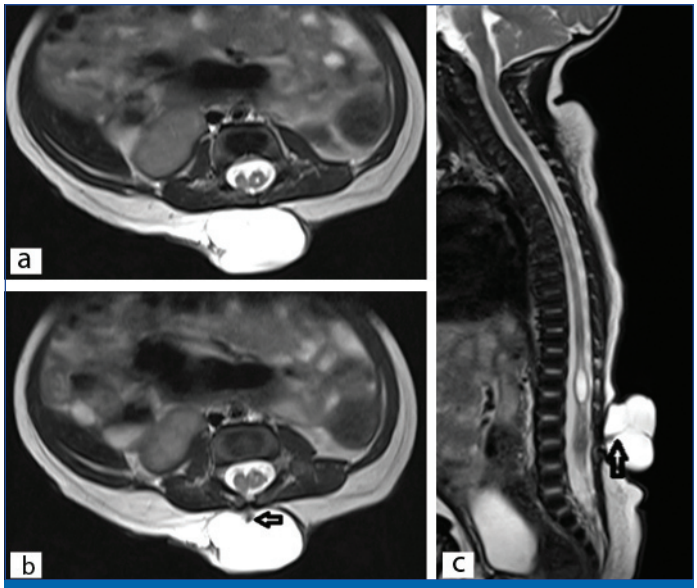

[Table/Fig-22]: Hemimyelomeningocele- axial T2 weighted image shows type 2 diastometamyelia with the right hemicord (arrow) seen ending within a myelomeningocele sac.

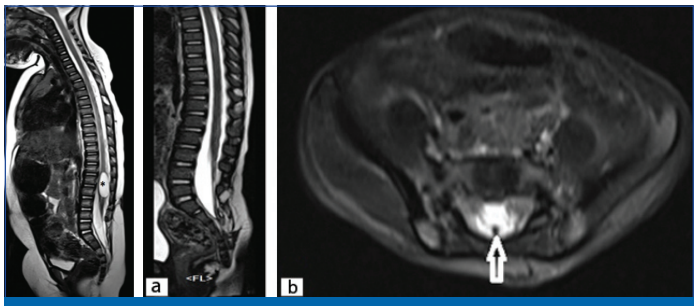

[Table/Fig-23]: Persistent terminal ventricle- T2 weighted sagittal image of lumbosacral spine showing cystic structure (*) at inferior aspect of conus medullaris, suggesting of persistent terminal ventricle. **[Table/Fig-24]:** Low lying tethered cord- Sagittal T2 weighted (a) and axial T2 STIR (b) images show low lying tethered cord with thickened filum terminale (arrow in b). (Images from left to right)

REFERENCES

[1] French BN. The embryology of spinal dysraphism. Clin Neurosurg. 1983;30:295-340.
[2] Rossi A, Cama A, Piatelli G, Ravegnani M, Biancheri R, Tortori-Donati P. Spinal dysraphism: MR imaging rationale. J Neuroradiol. 2004;31(1):03-24.
[3] Tortori-Donati P, Rossi A, Cama A. Spinal dysraphism: A review of neuroradiological features with embryological correlations and proposal for a new classification. Neuroradiology. 2000;42:471-91.
[4] Barkovich AJ. Pediatric neuroradiology, 4th ed. Philadelphia, PA: Lippincott Willims & Wilkins, 2011: pp. 857-916.
[5] Tortori-Donati P, Rossi A, Biancheri R (2005a) Brain malformations. In: Tortori-Donati P (ed) Pediatric neuroradiology. Springer, Berlin Heidelberg New York.
[6] Medical Research Council. MRC Vitamin Study Research Group. Prevention of neural tube defects: Results of the Medical Research Council vitamin study. Lancet. 1991;338:131-37.
[7] Medical Research Council. MRC randomized controlled trial use of multivitamins and folic acid for the prevention of recurrence of neural tube defects. Lancet. 1991;338:153-54.
[8] Text book of Pediatric surgery 7th Ed, Arnold G.Coran, N.Scott Adzick, Thomas M.Krummel, Jean martin laberge, Anthony Caldamone, Robert Shamberger Chapter 128 Pg 1673,1675.
[9] Kitzmiller JL, Buchanan TA, Kjos S, Combs CA, Ratner RE. Preconception care of diabetes, congenital malformations, and spontaneous abortions. Diabetes Care. 1996;19:514-41.
[10] Thunem NY, Lowry RB, Tucher BM, Medd BW. Birth prevalence and recurrence rates of neural tube defects in southern Alberta in 1970-1981. Can Med Assoc J. 1988;138:819-23.
[11] Moore K. Congenital Abnormalities of the Spine In: Coley BD, editor. Caffey's Pediatric Diagnostic Imaging. Philadelphia, PA: Elsevier Saunders; 2013. Pp. 449-60.
[12] Acharya UV, Pendharkar H, Varma DR, Pruthi N,Varadarajan S. Spinal dysraphism illustrated; Embroyology revisited. Indian J Radiol Imaging. 2017;27:417-26.
[13] Tortori-Donati P, Rossi A, Biancheri R, Cama A. Magnetic resonance imaging of spinal dysraphism. Top Magn Reson Imaging. 2001;12:375-409.
[14] Rossi A, Biancheri R, Cama A, Piatelli G, Ravegnani M, TortoriDonati P. Imaging in spine and spinal cord malformations. Eur J Radiol. 2004;50:177-200.
[15] Thompson D. Spinal dysraphic anomalies; classification, presentation and management. Paediatrics and Child Health. 2010;20:397-403.

[16] Dias MS, Walker ML. The embryogenesis of complex dysraphic malformations: A disorder of gastrulation? Pediatr Neurosurg. 1992;18:229-53.
[17] Tortori-Donati P, Fondelli MP, Rossi A, Raybaud CA, Cama A, Capra V. Segmental spinal dysgenesis: Neuroradiologic findings with clinical and embryologic correlation. AJNR Am J Neuroradiol. 1999;20:445-56.
[18] Estin D, Cohen AR. Caudal agenesis and associated caudal spinal cord malformations. Neurosurg Clin N Am. 1995;6:377-91.
[19] Rufener SL, Ibrahim M, Raybaud CA, Parmar HA. Congenital spine and spinal cord malformations-pictorial review. AJR Am J Roentgenol. 2010;194:S26-37.
[20] Zana E, Chalard F, Mazda K, Sebag G. An atypical case of segmental spinal dysgenesis. Pediatr Radiol. 2005;35:914-17.
[21] Harris CP, Dias MS, Brockmeyer DL, Townsend JJ, Willis BK, Apfelbaum RI. Neurenteric cysts of the posterior fossa: Recognition, management, and embryogenesis. Neurosurgery. 1991;29:893-97; discussion 897-898.
[22] Rufener S, Ibrahim M, Parmar HA. Imaging of congenital spine and spinal cord malformations. Neuroimaging Clin N Am. 2011;21:659-76.
[23] Simon JA, Olan WJ, Santi M. Intracranial neurenteric cysts: A differential diagnosis and review. Radiographics. 1997;17:1587-93.
[24] Pang D, Dias MS, Ahab-Barmada M. Split cord malformation: Part I: A unified theory of embryogenesis for double spinal cord malformations. Neurosurgery. 1992;31:451-80.
[25] Barkovich AJ, Edwards Ms, Cogen PH. MR evaluation of spinal dermal sinus tracts in children. AJNR Am J Neuroradiol. 1991;12:123-29.
[26] Naidich TP, McLone DG, Mutluer S. A new understanding of dorsal dysraphism with lipoma (lipomyeloschisis): Radiologic evaluation and surgical correction. AJR Am J Roentgenol. 1983;140:1065-78.
[27] Uchino A, Mori T, Ohno M. Thickened fatty filum terminale: MR imaging. Neuroradiology. 1991;33:331-33.
[28] Brown E, Matthes JC, Bazan C, Jinkins JR. Prevalence of incidental intraspinal lipoma of the lumbosacral spine as determined by MRI. Spine (Phila Pa 1976). 1994;19:833-36.
[29] Scotti G, Harwood-Nash DC, Hoffman HJ. Congenital thoracic dermal sinuses: Diagnosis by computer-assisted metrizamide myelography. J Comput Assist Tomogr. 1980;4(5):675-77.
[30] Naidich TP, Blaser SI, Delman BN. Congenital Anomalies of the Spine and Spinal Cord: Embryology and Malformations. In: Atlas SW eds. Magnetic Resonance Imaging of the Brain and Spine, 4th ed. Philadelphia: Lippincott Williams & Wilkins, 2009:1364-1447.
[31] Widjaja E, Whitby EH, Paley MN, Griffiths PD. Normal fetal lumbar spine on postmortem MR imaging. AJNR Am J Neuroradiol. 2006;27:553-59.
[32] Coleman LT, Zimmerman RA, Rorke LB. Ventriculus terminalis of the conus medullaris: MR findings in children. AJNR Am J Neuroradiol. 1995;16(7):1421-26.

PARTICULARS OF CONTRIBUTORS:
1. Senior Resident, Department of Radiology, ESIC Superspeciality Hospital, Hyderabad, Telangana, India.
2. Assistant Professor, Department of Radiology, ESIC Superspeciality Hospital, Hyderabad, Telangana, India.
3. Senior Resident, Department of Radiology, ESIC Superspeciality Hospital, Hyderabad, Telangana, India.

NAME, ADDRESS, E-MAIL ID OF THE CORRESPONDING AUTHOR:
Anurudh Kishore Vatti,
ESIC Superspeciality Hospital, Hyderabad, Telangana, India.
E-mail: anurudh.kishore@gmail.com

PLAGIARISM CHECKING METHODS: [Jain H et al.]
- Plagiarism X-checker: Sep 29, 2020
- Manual Googling: Feb 18, 2021
- iThenticate Software: Sep 10, 2021 (21%)

ETYMOLOGY: Author Origin

AUTHOR DECLARATION:
- Financial or Other Competing Interests: None
- Was Ethics Committee Approval obtained for this study? No
- Was informed consent obtained from the subjects involved in the study? Yes
- For any images presented appropriate consent has been obtained from the subjects. Yes

Date of Submission: **Sep 28, 2020**
Date of Peer Review: **Nov 28, 2020**
Date of Acceptance: **Feb 20, 2021**
Date of Publishing: **Oct 01, 2021**